Acteoside ameliorates diabetic kidney disease via regulating the activation of the PPARγ/β-catenin pathway

Yi-Hua Bai, Min Yang[*]**, Zhi-Jian Feng, Shuai Zheng**

Department of Nephrology, The Second Hospital Affiliated to Kunming Medical University, Kunming, Yunnan 650101 China

[*]Corresponding author, e-mail: miny524036@163.com

ABSTRACT: Diabetic kidney disease (DKD) is a common complication of diabetes. Acteoside is the main component of *Rehmannia glutinosa* leaves that shows renal protective effects. This study aimed to explore the protective role of acteoside on podocytes in DKD. Mouse podocyte cell line MPC-5 was stimulated with advanced glycation end products (AGEs) to establish an *in vitro* DKD model and, then, treated with or without acteoside. The expression levels of miR-27a, PPAR (peroxisome proliferator-activated receptor), and β-catenin were measured at 24 h and 48 h post-treatment. Sprague-Dawley rats were randomly divided into 5 groups: control; DKD; A-1 (DKD + low dose acteoside); A-2 (DKD + medium dose acteoside); and A-3 (DKD + high dose acteoside). The blood and urine biochemical indexes and the renal expressions of miR-27a, PPAR-1γ, and β-catenin were detected. Compared with the control group, the expressions of α-SMA, Snail-1, miR-27a, and β-catenin in AGE-stimulated cells were significantly higher. The effects of acteoside intervention significantly downregulated their expression in AGE-challenged group. The levels of PPARγ and synaptopodin in AGE-stimulated cells were significantly lower than those in the control group, whereas acteoside treatment significantly restored the expressions of these genes. Acteoside alleviated podocyte injury by downregulating miR-27a expression, rescuing the reduction of PPARγ, and inhibiting the activation of β-catenin signaling in the kidney tissues of DKD rats. Acteoside ameliorated podocyte injury in DKD by inhibiting the activation of PPARγ/β-catenin signaling pathway and this process might involve the regulation of miR-27a expression. Our findings suggest a therapeutic potential of acteoside in treating podocyte injury in DKD.

KEYWORDS: acteoside, miR-27a, PPARγ/β-catenin signaling, diabetic nephropathy

INTRODUCTION

Diabetic kidney disease (DKD) is a common complication of diabetes. In recent years, it has become a leading cause of end-stage renal disease in China [1]. Podocyte injury has been identified as a key event in the pathogenesis of DKD, resulting in the disruption of glomerular filtration barrier, podocyte foot process effacement and depletion [2]. The Wnt/β-catenin signaling pathway plays an important role in podocyte damage, and its increased activity has been observed in the podocytes of DKD patients and animal models [3]. The induction of Wnt/β-catenin signaling triggers the transcription of downstream targets, such as α-smooth muscle actin (α-SMA), snail-1, and c-myc [4]. Peroxisome proliferator-activated receptor gamma (PPARγ) is a member of the PPAR nuclear receptor family associated with diabetic kidney injury [5]. It has been

reported that the activation of PPARγ/β-catenin signaling aggravated podocyte injury in the kidneys of DKD patients [6, 7]. Some studies showed that the expression of PPARγ in obese animal models could be inhibited by the overexpression of microRNA-27a (miR-27a), which promoted the production of inflammatory factors [8, 9]. Also in DKD, PPARγ expression can be increased, and mesangial cell proliferation and fibrosis can be reduced by inhibiting the expression of miR-27a [10].

Acteoside is an extract obtained from *Rehmannia glutinosa* leaves and has been shown to ameliorate inflammation-induced mesangial cell injury in IgA nephropathy by regulating the chemotaxis and proliferation of Th22 lymphocytes [11]. The renal protective effect of acteoside was also observed in rats with puromycin nephropathy, in which acteoside alleviated puromycin-induced podocyte injury as evidenced by reduced proteinuria, restored

podocyte viability, and suppressed podocyte migration [12]. Thus, we hypothesized that acteoside might exert a renal protective effect on DKD.

In this study, the protective effects of acteoside against DKD injury and the role of PPARγ/β-catenin pathway were investigated using a rat model of streptozotocin (STZ)-induced DKD and an *in vitro* podocyte injury model.

MATERIALS AND METHODS

AGEs and acteoside

The advanced glycation end products (AGEs) were purchased from Sigma-Aldrich (St. Louis, USA). Acteoside powder was provided by MeiDaKang Pharmaceutical Co., Ltd (Sichuan, China), which contained acteoside (70%) and the structural isoforms of acteoside, including hydroxyacteoside, methoxyacteoside, isoacteoside, and cisacteoside (30%) [13, 14]. The doses of acteoside used in this study were selected as previously described [12].

Cell culture

MPC-5 cells (Catalog no. 5045479161-01) were purchased from the Yuxi Biotechnology Co., Ltd (Jiangyin, China); cultured in DMEM, containing 10% fetal bovine serum, 100 U/ml of penicillin, and 100 U/ml of streptomycin, and incubated in a 5% CO_2 incubator at 37 °C. The culture medium was replaced every 2–3 weeks. Then, cells were passaged, seeded in 6-well plates and divided into 5 groups: (1) control (normal, remained untreated); (2) AGE-induced podocyte injury model (DKD); (3) DKD + acteoside low dose (A-1, 100 mmol/l); (4) DKD + acteoside medium dose (A-2, 150 mmol/l); and (5) DKD + acteoside high dose (A-3, 200 mmol/l). When cells reached 80% confluence, the culture medium was replaced by serum-free DMEM. AGEs at 200 µg/ml was added into designated groups for 24 h or 48 h. Each group was prepared in triplicate.

Annexin V-FITC/PI apoptosis detection

The adherent cells were digested with EDTA-free trypsin, collected, and centrifuged at 2000 rpm for 5–10 min. Cell pellets were re-suspended in phosphate-buffered saline (PBS, 4 °C), washed, and centrifuged at 2000 rpm for 5–10 min. Then, 300 µl binding buffer was added for suspension followed by a 15-min incubation with 5 µl of Annexin V-FITC at room temperature. A volume of 5 µl propidium iodide (PI) was added for staining 5 min before sample loading.

Animal study

Thirty healthy Sprague Dawley rats (150–200 g) were randomly divided into 5 groups (n=5/group): control group (C, remained untreated); DKD group (DKD); DKD + low dose of 10 mg/kg acteoside (A-1); DKD + medium dose of 20 mg/kg acteoside (A-2); and DKD + high dose of 40 mg/kg acteoside (A-3). The STZ administration was performed as previously published [15]. Rats in the DKD group were fed with high fat-diet for 4 weeks, and then intraperitoneally injected with STZ solution (35 mg/kg/day) for 4 days. The blood glucose of each rat was measured bi-weekly since the beginning of high-fat diet intervention. Starting from the first day of STZ injection, blood glucose was monitored every three days. At 72 h after the last injection, blood samples were collected from the tail vein for the detection of fasting blood glucose. Rats with fasting blood glucose of >16.7 mmol/l twice were selected as the diabetic model. Diabetic rats showing >50% increase in 24 h urine volume and 24 h urine protein excretion were considered as successful establishment of DKD rats[16]. Furthermore, the 24-h urine samples in the C and DKD groups were collected to detect urine protein. The acteoside powder was dissolved with normal saline and intraperitoneally injected into rats, once a day, for 5 days. At 2 weeks after the last injection, the 24-h urine of rats was collected with metabolic cages. Then the animals were anesthetized with pentobarbital, sacrificed, and peripheral blood and kidney tissues were harvested.

Blood and urine specimen test

Blood glucose was measured using a Bayer blood glucose meter. The corresponding kits were used to detect blood urea nitrogen (LM-12028, LMAIBio, Shanghai, China), serum creatinine (LM-12068, LMAIBio), random urinary protein, and urinary creatinine (GD-vN9908, Guduo Biotechnology, Shanghai, China). The 24-h urinary protein was detected using an automatic biochemical detector (7170A, Japan).

RT-PCR

A Trizol kit (TransGen Biotech, China; H10318) was used to extract the RNA from collected cells. RNA reverse transcription was performed using a reverse transcriptase kit (Promega), and the reaction system was 20 µl. The primer sequences were shown in Table S1. Reaction conditions: 95 °C for 3 min, 95 °C for 30 s, and 55 °C for 20 s for 40 cycles; then,

72 °C for 20 s. Dissolution curve steps: 95 °C for 15 s, 60 °C for 15 s, warming up for 20 min, and 95 °C for 15 s.

The total RNA from kidney tissues was extracted using Trizol RNA extract. RNA reverse transcription was performed using a HiScript® II Reverse Transcriptase kit (Vazyme). PCR amplification was performed using a ChamQTM SYBR® qPCR Master Mix fluorescence quantitative kit (Vazyme). The primer sequences were shown in Table S2. Reaction conditions: Stage 1 initial denaturation, 95 °C for 30 s; Stage 2 denaturation, 95 °C for 10 s; annealing/extension 60 °C for 30 s, 40 cycles.

Western blot

Cell lysates were prepared and the protein concentration was measured using a bicinchoninic acid (BCA) protein assay kit (Beyotime Biotechnology). The protein (30 µg) was separated by SDS-PAGE and transferred onto a polyvinylidene fluoride (PVDF) membrane by electrophoresis with 15 mA of constant current power. Next, cell protein samples were blocked with 5% skim milk powder for 2 h, and later incubated with the following primary antibodies: PPARγ (1:1000 dilution, Ab-mart, Berkeley Heights, USA) and β-catenin (1:500 dilution, Huagene, Shanghai, China) at 4 °C overnight. Then, the membrane was washed with TBST, added with a secondary antibody (1:2000), and incubated for 2 h. The membrane was colored, exposed, and scanned to obtain the films. With β-actin (Catalog no. 1854-s, HuaAn, Hangzhou, China) as the internal control, the expressions of PPARγ and β-catenin were detected.

The kidney tissue specimens were levigated and homogenized, and the tissue protein was extracted using phenylmethanesulfonyl fluoride/PMSF solution. The protein concentration was determined by BCA, and 30 µg were separated by gel electrophoresis. The protein was, then, transferred onto a membrane, blocked with 5% dried skimmed milk, and incubated with the following primary antibodies (1:1000 dilution) at 4 °C overnight: αSMA (A7637, Abclonal, Woburn, USA); Snail (A11794, Abclonal); β-catenin (A2090, Abclonal); Synaptopodin (A8484, Abclonal); and PPAR-γ (YPT3836, ImmunoWay, Plano, USA). Membranes were, later, washed with TBST and incubated with a secondary antibody (1:5000, Abclonal) at room temperature for 1 h. After being rinsed with TBST, membranes were colored with enhanced chemiluminescence (ECL). The Bio-rad chemiluminescence gel imaging device was used for band exposure and im-

age preservation. Beta-actin (Catalog no. 1854-s, HuaAn, Hangzhou, China) was used as an internal control.

Immunohistochemistry

Cells and kidney tissues were fixed with 2.5% glutaraldehyde phosphate buffer, embedded in epoxy resin, and sectioned. Immunohistochemical staining was used to assess the expression of α-SMA, Snail-1, synaptopodin, β-catenin, or PPAR-γ (1:100 dilution, Maxim, Fuzhou, China). Positive staining was defined as brown or brownish-yellow stains in the cytoplasm under light microscope. An automatic digital imaging system was used for imaging. Then, the expression situations were analyzed using ImageJ software, and 10 discontinuous visual fields were evaluated.

Statistical analysis

All samples were analyzed in triplicate. The cell culture experiments were repeated three times. Data were analyzed using SPSS 17.0. Normal distributions of quantitative data were expressed as mean ± standard deviation. Repeated measurement data were analyzed using repeated measures analysis of variance (ANOVA). Comparison among groups was conducted using one-way ANOVA. $p < 0.05$ was considered statistically significant; * indicates significant difference when compared with the control group at the same time point, * $p < 0.05$, ** $p < 0.01$; # indicates significant difference when compared with the DKD group at the same time point, # $p < 0.05$, ## $p < 0.01$.

RESULTS

Acteoside suppressed apoptosis and regulated the RNA expressions of miR-27a, PPAR-γ, and β-catenin in AGE-induced MPC-5 cells

Cells treated with AGEs, when compared with the control group, showed a significantly higher apoptosis rate at both 24 h and 48 h post-treatments ($p < 0.01$). However, the intervention of acteoside in A-1, A-2, and A-3 significantly suppressed AGE-stimulated apoptosis in MPC-5 podocytes ($p < 0.01$, Fig. 1A). Compared with the control, the expression of miR-27a in MPC-5 cells was significantly increased by AGE stimulation at both 24 h and 48 h after acteoside treatment ($p < 0.05$). The treatment of acteoside at all doses significantly decreased the miR-27a level at both time points ($p < 0.05$). In A-3 group, the level of miR-27a was similar to that in the control group ($p > 0.05$) (Fig. 1B). AGE-treated
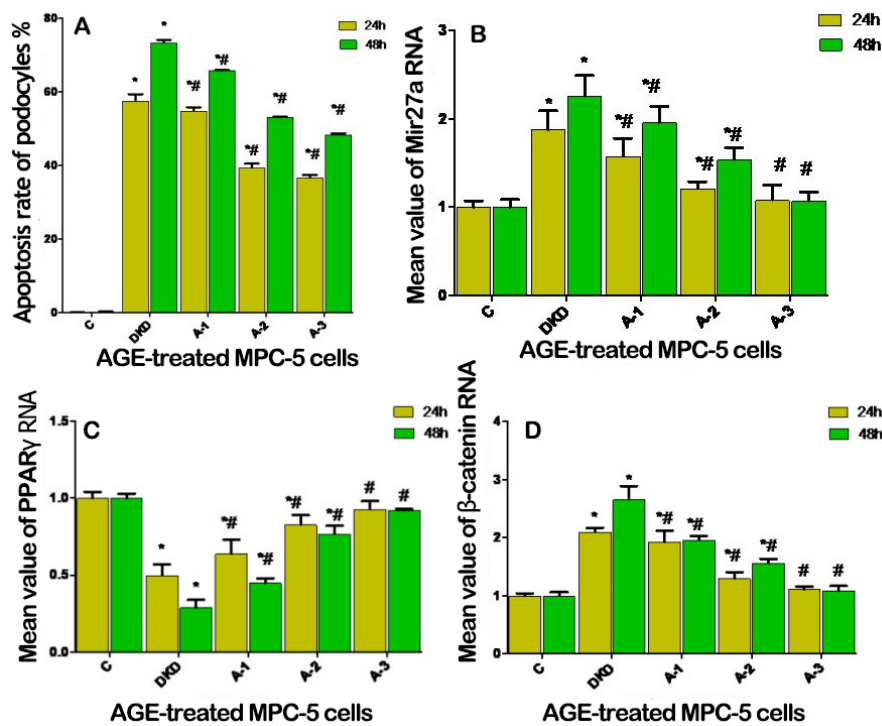
Fig. 1 Effects of acteoside on the apoptosis rates and the expressions of miR-27a, PPARγ and β-catenin in AGE-induced MPC-5 cells. MPC-5 cells received designated doses of acteoside for 24 or 48 h followed by the detection of (A) apoptosis rate and the measurements of (B) miR-27a, (C) PPARγ, and (D) β-catenin expressions.
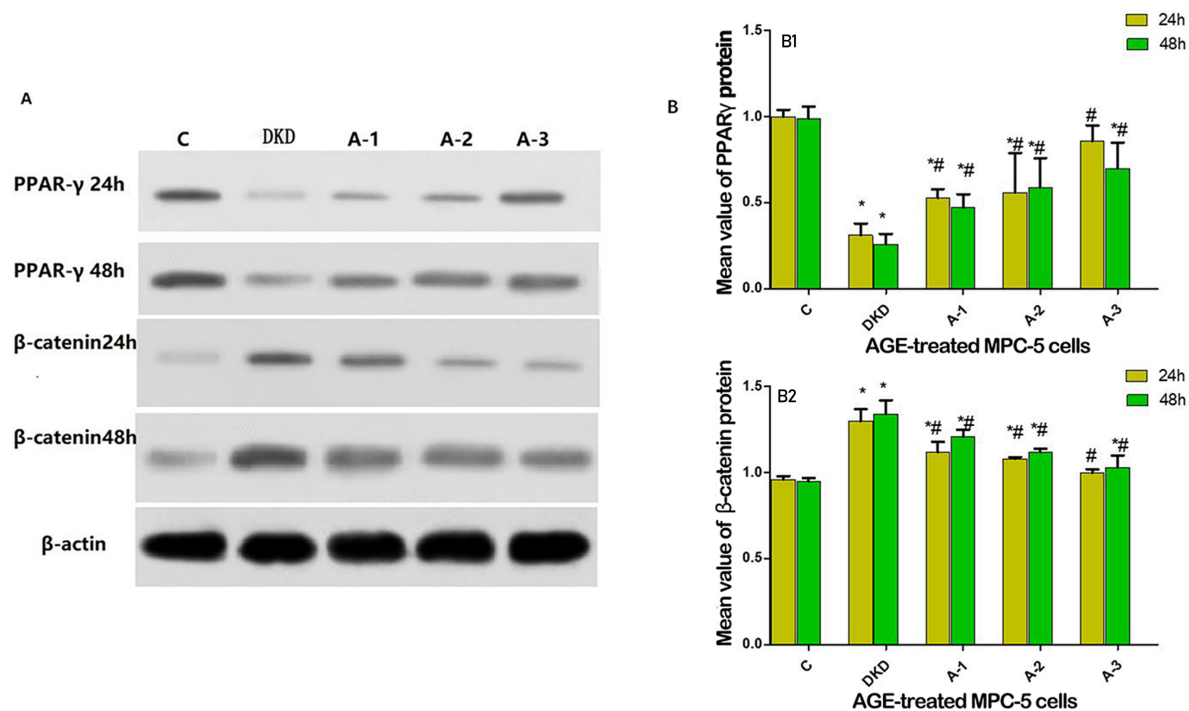

Fig. 2 Effects of acteoside on the protein expressions of PPARγ and β-catenin in AGE-treated MPC-5 cells. The expressions of PPARγ and β-catenin in MPC-5 cells were measured using Western blot at 24 h or 48 h post-treatment.

cells showed significantly reduced expression of PPARγ as compared with the control group ($p < 0.05$), whereas acteoside intervention successfully restored PPARγ expression at all doses ($p < 0.05$) (Fig. 1C). The robust effect of acteoside was observed when the high concentration (200 mmol/l) was applied. The level of β-catenin was significantly induced by AGE treatment ($p < 0.05$) but suppressed by acteoside at all doses ($p < 0.05$). The levels of β-catenin between the A-3 group and the control showed no statistical significance ($p > 0.05$, Fig. 1D). Consistently, AGE stimulation inhibited the protein expression of PPARγ and induced the level of β-catenin in MPC-5 cells in comparison with the control ($p < 0.05$). The intervention of acteoside at all doses effectively promoted the levels of PPARγ and downregulated the β-catenin expression in injured MPC-5 cells ($p < 0.05$, Fig. 2).

Effects of acteoside on the protein expression of α-SMA, Snail-1, and synaptopodin in AGE-treated podocytes

Next, we performed immunohistochemistry in cells at 24 h and 48 h after acteoside treatment. The levels of α-SMA and Snail-1 in DKD group were significantly higher than those in the control ($p < 0.05$). The treatment of acteoside at all concentrations effectively downregulated AGE-induced expressions of α-SMA and Snail-1 ($p < 0.05$). The synaptopodin level in injured podocytes, however, was significantly lower than that in the control group ($p < 0.05$). Acteoside at all doses (A-1, A-2, and A-3) significantly upregulated synaptopodin expression in AGE-treated cells ($p < 0.05$, Table 1).

Effects of acteoside on blood and urine biochemical indicators in diabetic rats

To explore the effects of acteoside on DKD *in vivo*, an animal model of STZ-induced diabetes was established. When compared with the control group ($p < 0.05$), diabetic rats showed significantly higher levels of blood glucose, urea nitrogen, serum creatinine, 24-h urinary protein, and the urinary protein-to-creatinine ratio. Acteoside at medium and high doses (A-2 and A-3) efficiently decreased all blood and urine biochemical indicators in diabetic rats ($p < 0.05$, Table 2).

Effects of acteoside on the expressions of α-SMA, Snail-1, synaptopodin, miR-27a, PPAR-γ, and β-catenin in rats with diabetic kidney injury

DKD group showed significant increased levels of α-SMA, Snail-1, miR-27a, and β-catenin; and de-creased expressions of synaptopodin and PPAR-γ when compared with the control ($p < 0.05$). In the A-2 and A-3 groups, the renal RNA expressions of α-SMA, Snail-1, miR-27a, and β-catenin were effectively downregulated; and the levels of synaptopodin and PPAR-γ were greatly increased ($p < 0.05$, Fig. 3). When compared with the control, rats with diabetes showed significantly higher protein expressions of α-SMA, Snail-1, and β-catenin, whereas the levels of synaptopodin and PPAR-γ were significantly decreased. The treatment of high dose acteoside (200 mmol/l) showed the robust effect on suppressing the induction of α-SMA, Snail-1, and β-catenin; and restoring the levels of synaptopodin and PPAR-γ ($p < 0.05$, Fig. 4). Consistently, immunohistochemistry data showed that the renal expressions of α-SMA, Snail-1, and β-catenin in the DKD group were higher than those in the control. However, the expressions of PPARγ and synaptopodin were lower in DKD when compared with the control. The intervention of acteoside effectively reversed diabetes-induced aberrant expressions of these proteins (Fig. 5).

DISCUSSION

Acteoside is the main compound of *Rehmannia glutinosa*. It belongs to phenylethanoid glycosides whose effects are known for nourishing the Yin, tonifying the kidney, and improving intestinal flora imbalance in diabetic nephropathy animals [14, 17, 18]. Previous studies revealed that the expression of calcineurin is significantly increased in kidney tissues of STZ-induced early diabetic animal models [19, 20], while another study demonstrated that acteoside had the effect of inhibiting the expression of calcineurin in the kidney of diabetic nephropathy animals [21]. This indirectly suggests that acteoside may be a potential effective drug for DKD treatment.

MiRNA is an endogenous single-stranded small RNA molecule, which participates in the regulation of gene expression, and influences various biological processes [22–24]. The plasma level of miR-27a can reflect the degree of renal tubulointerstitial fibrosis in DKD, and the mechanism is that miR-27a inhibits PPARγ expression and activates the TGF-β/Smad signaling pathway [25–27]. A study also confirmed that in DKD, β-catenin activation was one of the mechanisms that mediated podocyte injury [28]. Therefore, miR-27a, PPARγ and β-catenin all play important roles in the pathogenesis of DKD. Meizhou Zhan et al [6] confirmed that the upregulation of miR-27a and activation of the PPARγ/β-catenin pathway were mechanisms leading to the
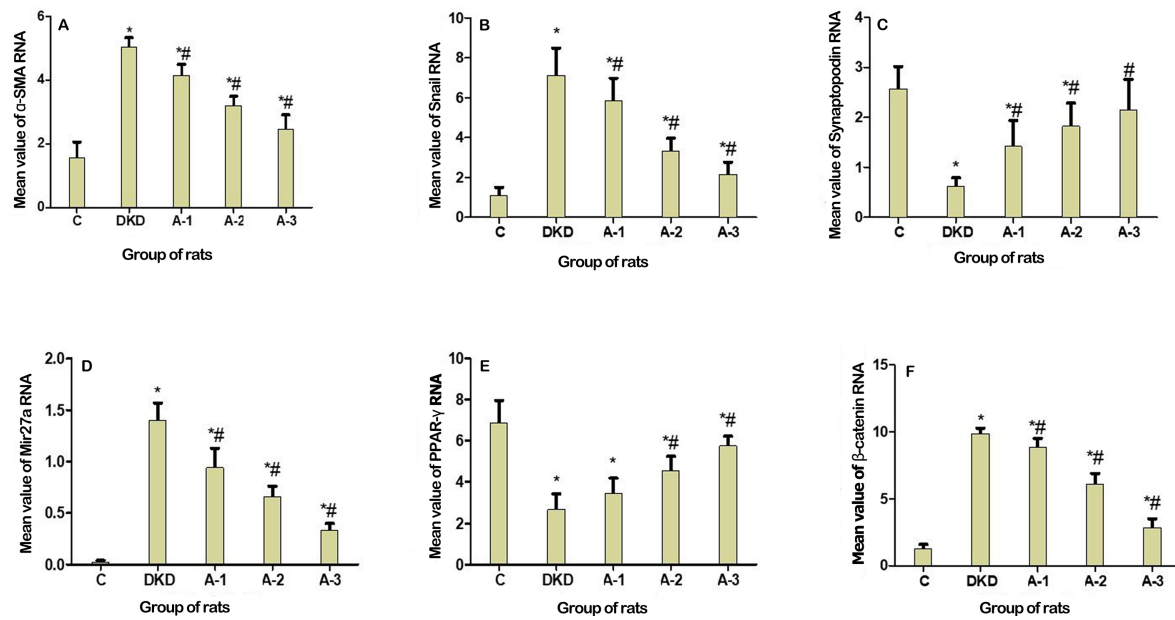
Fig. 3 Effects of acteoside on the RNA expressions of α-SMA, Snail-1, synaptopodin, miR-27a, PPAR-γ, and β-catenin in rats with STZ-induced DKD. Rats received designated doses of acteoside and their kidney tissues were collected. The expressions of α-SMA, Snail-1, synaptopodin, miR-27a, PPAR-γ, and β-catenin were measured using RT-PCR.
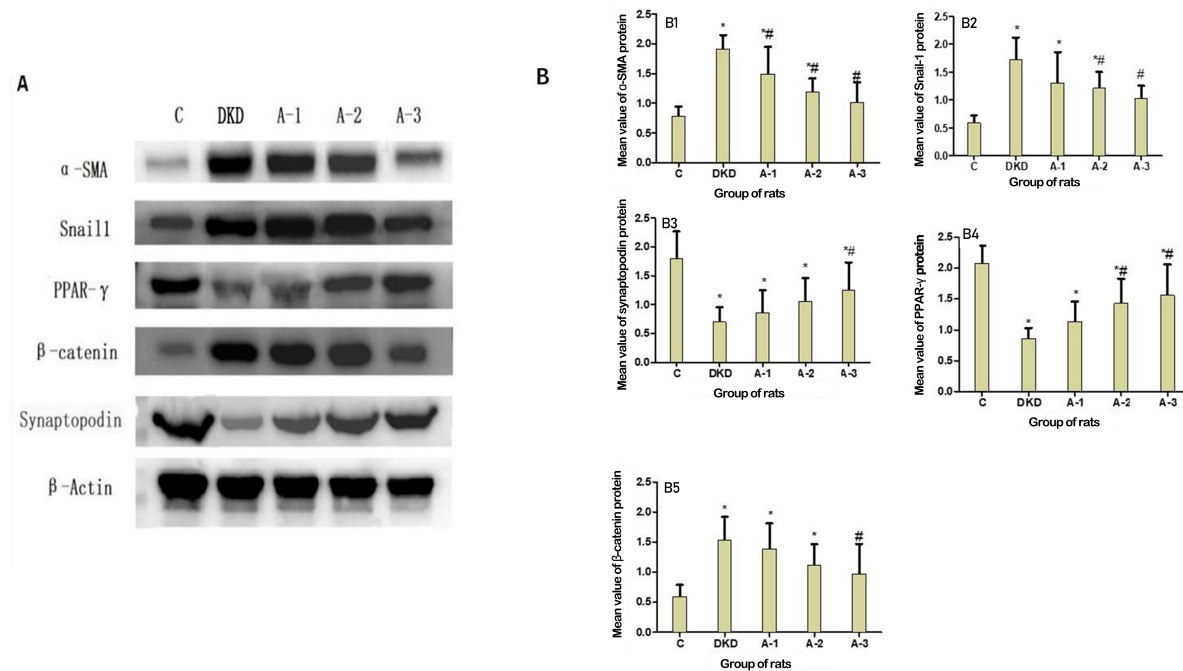

Fig. 4 Effects of acteoside on the protein expressions of α-SMA, Snail-1, PPAR-γ, β-catenin, and synaptopodin in DKD rats. Rat kidney tissues were harvested after the treatment; and the protein expressions of α-SMA, Snail-1, PPAR-γ, β-catenin, and synaptopodin were assessed using Western blot.

Table 1 The integral optical density (IOD) values of all groups of cells measured by immunohistochemical staining.

Group	24 h			48 h		
	α-SMA	Snail-1	Synaptopodin	α-SMA	Snail-1	Synaptopodin
C	15.33 ± 2.08	13.00 ± 1.00	21.63 ± 1.34	12.00 ± 1.00	13.33 ± 0.58	22.35 ± 0.95
DKD	$45.00 \pm 7.55^*$	$30.33 \pm 1.53^*$	$15.37 \pm 0.38^*$	$35.00 \pm 8.19^*$	$35.67 \pm 2.08^*$	$14.45 \pm 0.96^*$
A-1	$25.67 \pm 3.79^{*\#}$	$18.33 \pm 2.52^{*\#}$	$17.21 \pm 0.28^{*\#}$	$20.33 \pm 2.31^{*\#}$	$23.00 \pm 1.73^{*\#}$	$16.68 \pm 0.55^{*\#}$
A-2	$14.67 \pm 1.53^{\#}$	$18.67 \pm 2.52^{*\#}$	$18.09 \pm 0.49^{*\#}$	$14.67 \pm 2.08^{\#}$	$15.67 \pm 1.16^{\#}$	$18.17 \pm 0.92^{*\#}$
A-3	$12.33 \pm 0.58^{\#}$	$14.67 \pm 0.58^{\#}$	$21.97 \pm 1.90^{\#}$	$11.33 \pm 1.16^{\#}$	$15.67 \pm 1.16^{\#}$	$21.64 \pm 0.71^{\#}$

* $p < 0.05$ compared with the control group at the same time point.
$^{\#}$ $p < 0.05$ compared with the DKD group at the same time point.

Table 2 The body weight, blood and urine biochemical indicators in rats.

Group	n	Body weight (g)	Blood glucose (mmol/l)	Urea nitrogen (mmol/l)	Creatinine (μmol/l)	Urine protein quantitation for 24 h (g/24 h)	Urine protein/ creatinine (mg/g Cr)
C	5	198.66 ± 17.93	5.18 ± 0.49	5.47 ± 0.16	38.71 ± 4.70	0.26 ± 0.11	17.11 ± 2.30
DKD	5	$361.67 \pm 50.91^*$	$31.98 \pm 2.90^*$	$12.45 \pm 0.95^*$	$66.20 \pm 1.94^*$	$4.66 \pm 1.01^*$	$1204.02 \pm 28.90^*$
A-1	5	$357.03 \pm 20.40^*$	$24.24 \pm 3.09^{*\#}$	$11.51 \pm 1.74^*$	$62.01 \pm 1.48^{*\#}$	$3.48 \pm 0.77^{*\#}$	$1193.02 \pm 24.42^*$
A-2	5	$386.48 \pm 15.09^*$	$20.36 \pm 3.64^{*\#}$	$10.14 \pm 1.70^{*\#}$	$61.77 \pm 0.84^{*\#}$	$1.92 \pm 0.69^{*\#}$	$836.67 \pm 27.96^{*\#}$
A-3	5	$339.14 \pm 77.28^*$	$17.98 \pm 1.08^{*\#}$	$9.99 \pm 1.13^{*\#}$	$58.35 \pm 3.56^{*\#}$	$1.13 \pm 0.25^{*\#}$	$551.60 \pm 13.31^{*\#}$

* $p < 0.05$ compared with the control group. $^{\#}$ $p < 0.05$ compared with the DKD group.

aggravation of podocyte injury in DKD. Thus, miR-27a may be a new potential for DKD treatment.

In our study, AGEs were used to induce podocyte injury modeling. The apoptosis rate of podocytes in AGE-treated cells was significantly higher than that in the control group, while acteoside intervention significantly reduced the apoptosis of AGEs-injured cells at 24 h and 48 h after treatment. Compared to the control group, the expression levels of miR-27a, PPARγ and β-catenin in the DKD group were significantly increased. After the incubation with acteoside for 24 h and 48 h, the expressions of miR-27a and β-catenin were greatly decreased and the level of PPARγ was restored in AGE-treated podocytes. Further immunohistochemical staining showed that acteoside significantly decreased the expressions of α-SMA and Snail-1, but elevated the level of synaptopodin in MPC-5 cells. α-SMA and snail-1 are the two downstream targets of the Wnt/β-catenin signaling pathway [29]. Synaptopodin has been identified as a classical podocyte-specific marker [30]. Our findings suggested that acteoside alleviated AGE-induced podocyte injury via suppressing the expression of miR-27a and the activation of Wnt/β-catenin signaling pathway. We further explored the therapeutic effect of acteoside on DKD *in vivo*. The levels of proteinuria and serum creatinine in diabetic rats were alleviated by

acteoside at different doses. Consistent with the *in vitro* data, the treatment of acteoside successfully reversed diabetes-induced aberrant expressions of miR-27a, α-SMA, Snail-1, β-catenin, PPARγ, and synaptopodin in rats with STZ-induced diabetes. The most robust therapeutic effect was observed in the A-3 group.

There were limitations in the present study. First, the effect of acteoside on the levels of blood pressure, blood lipids, and HbA1c were not explored. Also, the overexpression, or silencing, of miR-27a was not further verified; and the indicators were not detected at more time points in the animal experiments. Further investigations are needed to elucidate the molecular mechanisms of acteoside on the protective effect in DKD.

CONCLUSION

Podocyte injury plays an important role in DKD development. Our results demonstrated that acteoside intervention alleviated podocyte injury both *in vitro* and *in vivo*, by decreasing podocyte apoptosis, downregulating miR-27a expression, rescuing the reduction of PPARγ, and inhibiting the activation of β-catenin signaling. These results suggested a therapeutic potential of acteoside in alleviating podocyte injury in DKD, subsequently reducing proteinuria and protecting kidney function.
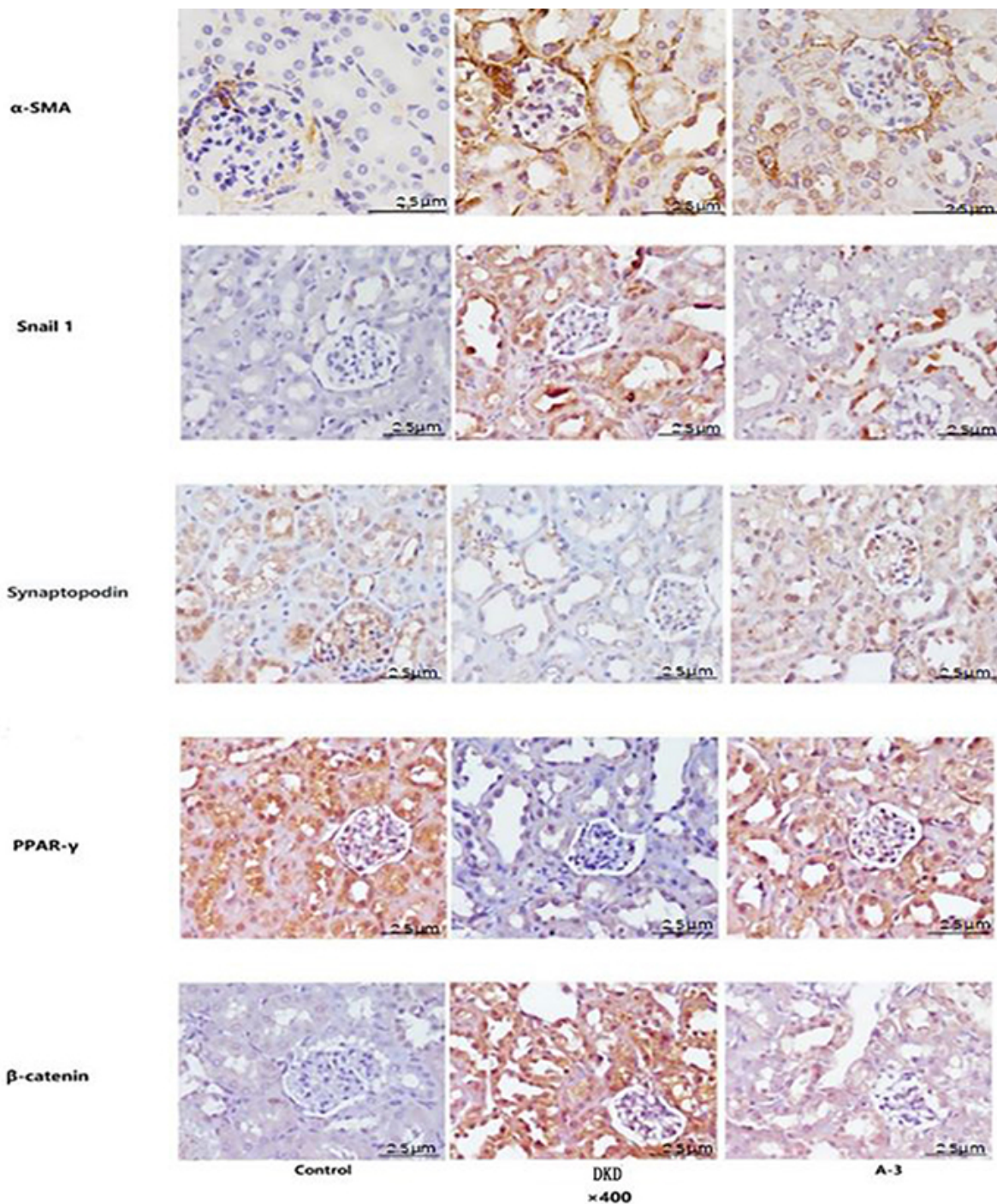
Fig. 5 Immunohistochemical staining of rat kidney tissues. Sectioned rat kidney tissues were stained with α-SMA, Snail-1, synaptopodin, PPAR-γ, and β-catenin using immunohistochemistry.

Appendix A. Supplementary data
Supplementary data associated with this article can be found at http://dx.doi.org/10.2306/scienceasia1513-1874.2021.034.

REFERENCES

1. Zhang L, Long J, Jiang W, Shi Y, He X, Zhou Z, Li Y, Yeung RO, et al (2016) Trends in chronic kidney disease in China. *N Engl J Med* **375**, 905–906.
2. Lin JS, Susztak K (2016) Podocytes: The weakest link in diabetic kidney disease? *Curr Diab Rep* **16**, ID 45.
3. Kato H, Gruenwald A, Suh JH, Miner JH, Barisoni-Thomas L, Taketo MM, Faul C, Millar SE, et al (2011) Wnt/β-catenin pathway in podocytes integrates cell adhesion, differentiation, and survival. *J Biol Chem* **286**, 26003–26015.
4. Fernández-Sánchez ME, Barbier S, Whitehead J, Béalle G, Michel A, Latorre-Ossa H, Rey C, Fouassier L, et al (2015) Mechanical induction of the tumorigenic β-catenin pathway by tumor growth pressure. *Nature* **523**, 92–95.
5. Zhang M, Yuan H, Li C, Li C (2017) The impact of peroxisome proliferator-activated receptor gamma and its interaction with abdominal obesity on diabetic nephropathy in Chinese Han. *Nephron* **135**, 224–230.
6. Zhou Z, Wan J, Hou X, Geng J, Li X, Bai X (2017) MicroRNA-27a promotes podocyte injury via PPARγ-mediated β-catenin activation in diabetic nephropathy. *Cell Death Dis* **8**, e2658.
7. Pattarayan D, Sivanantham A, Krishnaswami V, Loganathan L, Palanichamy R, Natesan S, Muthusamy K, Rajasekaran S (2018) Tannic acid attenuates TGF-beta1-induced epithelial-to-mesenchymal transition by effectively intervening TGF-beta signaling in lung epithelial cells. *J Cell Physiol* **233**, 2513–2525.
8. Yao F, Yu Y, Feng L, Li J, Zhang M, Lan X, Yan X, Liu Y, et al (2017) Adipogenic miR-27a in adipose tissue upregulates macrophage activation via inhibiting PPARγ of insulin resistance induced by high-fat diet-associated obesity. *Exp Cell Res* **355**, 105–112.
9. Sutariya B, Saraf M (2017) Betanin, isolated from fruits of *Opuntia elatior* mill attenuates renal fibrosis in diabetic rats through regulating oxidative stress and TGF-β pathway. *J Ethnopharmacol* **198**, 432–443.
10. Wu L, Wang Q, Guo F, Ma X, Ji H, Liu F, Zhao Y, Qin G (2016) MicroRNA-27a induces mesangial cell injury by targeting of PPARγ, and its *in vivo* knockdown prevents progression of diabetic nephropathy. *Sci Rep* **6**, ID 26072.
11. Gan L, Li X, Zhu M, Chen C, Luo H, Zhou Q (2018) Acteoside relieves mesangial cell injury by regulating Th22 cell chemotaxis and proliferation in IgA nephropathy. *Ren Fail* **40**, 364–370.
12. Ding FR, Si N, Bian BL, Ding J (2018) The effect of acteoside on puromycin nephropathy and podocyte injury model. *Chin J Nephrol* **34**, 30–35. [in Chinese]
13. Feng B, Song Y, Xu Q, Xu P, Zeng Q, Shan B, Liu K, Su D (2018) Simultaneous determination of savaside A, acteoside, and isoacteoside in rat plasma by UHPLC-MS/MS: Comparative pharmacokinetic and bioavailability characteristics of *Monochasma savatieri* via different routes of administration. *J Sep Sci* **41**, 4408–4418.
14. Dai XX, Su SL, Cai HD, Wei DD, Zheng TY, Zhu ZH, Yan H, Shang EX, et al (2017) Comparative pharmacokinetics of acteoside from total glycoside extracted from leaves of *Rehmannia* and *Dihuangye* total glycoside capsule in normal and diabetic nephropathy rats. *Biomed Chromatogr* **31**, e4013.
15. Guo YZ, Du J, Li XM, Feng XZ, Guo W (2017) Effect of *Coptis chinensis* on expression of nf-κb and ppar-γ in kidney of diabetic nephropathy rats. *World Chin Med* **12**, 884–887. [in Chinese]
16. Lei Z, Luo R, Dong X, Zhong X (2005) Establishment of stz-induced diabetic nephropathic rat model. *Zhongguo Shi Yan Dong Wu Xue Bao* **13**, 163–165.
17. Breyer MD, Kretzler M (2018) Novel avenues for drug discovery in diabetic kidney disease. *Expert Opin Drug Discov* **13**, 65–74.
18. Matsui F, Babitz SA, Rhee A, Hile KL, Zhang H, Meldrum KK (2017) Mesenchymal stem cells protect against obstruction-induced renal fibrosis by decreasing STAT3 activation and STAT3-dependent MMP-9 production. *Am J Physiol Renal Physiol* **312**, F25–F32.
19. Barzegar-Fallah A, Alimoradi H, Razmi A, Dehpour AR, Asgari M, Shafiei M (2015) Inhibition of calcineurin/NFAT pathway plays an essential role in renoprotective effect of tropisetron in early stage of diabetic nephropathy. *Eur J Pharmacol* **767**, 152–159.
20. Loeffler I, Liebisch M, Allert S, Kunisch E, Kinne RW, Wolf G (2018) FSP1-specific SMAD2 knockout in renal tubular, endothelial and interstitial cells reduces fibrosis and epithelial-to-mesenchymal transition in murine STZ-induced diabetic nephropathy. *Cell Tissue Res* **372**, 115–133.
21. Motojima H, Villareal MO, Iijima R, Han J, Isoda H (2013) Acteoside inhibits type I allergy through the down-regulation of Ca/NFAT and JNK MAPK signaling pathways in basophilic cells. *J Nat Med* **67**, 790–798.
22. Reinke CA, Carthew RW (2008) BMP signaling goes posttranscriptional in a microRNA sort of way. *Dev Cell* **15**, 174–175.
23. Schafer S, Viswanathan S, Widjaja AA, Lim WW, Moreno-Moral A, DeLaughter DM, Ng B, Patone G, et al (2017) IL-11 is a crucial determinant of cardiovascular fibrosis. *Nature* **552**, 110–115.
24. Chen M, Zhao F, Wang Z, Lang H, Zhang K, Zhang T, Wang R, Shi P, et al (2020) Low-expression of microRNA-203a in mid-gestational human fetal ker-

atinocytes contributes to cutaneous scarless wound healing by targeting Tenascin-C. *ScienceAsia* **46**, 133–141.

25. Hou X, Tian J, Geng J, Li X, Tang X, Zhang J, Bai X (2016) MicroRNA-27a promotes renal tubulointerstitial fibrosis via suppressing PPARγ pathway in diabetic nephropathy. *Oncotarget* **7**, 47760–47776.

26. Gheith O, Farouk N, Nampoory N, Halim MA, Al-Otaibi T (2015) Diabetic kidney disease: Worldwide difference of prevalence and risk factors. *J Nephropharmacol* **5**, 49–56.

27. Gilbert RE (2017) Proximal tubulopathy: Prime mover and key therapeutic target in diabetic kidney disease. *Diabetes* **66**, 791–800.

28. Wan J, Hou X, Zhou Z, Geng J, Tian J, Bai X, Nie J (2017) WT1 ameliorates podocyte injury via repression of EZH2/β-catenin pathway in diabetic nephropathy. *Free Radic Biol Med* **108**, 280–299.

29. Fernández-Sánchez ME, Barbier S, Whitehead J, Béalle G, Michel A, Latorre-Ossa H, Rey C, Fouassier L, et al (2015) Mechanical induction of the tumorigenic β-catenin pathway by tumor growth pressure. *Nature* **523**, 92–95.

30. Sekulic M, Pichler Sekulic S (2013) A compendium of urinary biomarkers indicative of glomerular podocytopathy. *Patholog Res Int* **2013**, ID 782395.

Appendix A. Supplementary data

Table S1 The primer sequences for RT-PCR of the RNA from collected cells.

Primer	Sequence
GAPDH-F	ACAGCAACAGGGTGGTGGAC
GAPDH-R	TTTGAGGGTGCAGCGAACTT
PPARγ-F	TGATATCGACCAGCTGAA-CC
PPARγ-R	ATGGCCACCTCT-TTGCTCT
β-catenin-F	ATGTGGTCACCTG-TGCAGCT
β-catenin-R	GGCTCAGTGATGTCTTCCCT
miR-27a	GGCATTC-ACAGTGGCTAAGT

Table S2 The primer sequences for RT-PCR of the total RNA from kidney tissues.

Primer	Sequence
GAPDH-F	ACTGAGAGCAAGAGAGAGGC
GAPDH-R	TTGTTATGGGGTCTGGGATGG
Snail 1-F	AGCCCA-ACTAGCGAGCTG
Snail-1-R	CCAGGAGAGTCCCAGATG
PPARγ-F	CCCTGCAAAGCA-TTTGTAT
PPARγ-R	ACTGGCACCCTTGAAAAATG
miR-27a	AGGG-CTTAGCTGCTTGTGAGCA
synaptopodin-F	CACCACAGCAGCCTCTAACA
synaptopodin-R	TGCTG-GACCTCACTTCCTCT
β-catenin-F	GCTTC TGTTGCCCTTCTCTCTCTCTC
β-catenin-R	TGGACGCTCTTTCCAACT
α-SMA-F	ACTGGGACGACATGGA-AAAG
α-SMA-R	CATCTCCAGAGTCCAGCAGCAGCAGCACACACACAGCACACACA